



# Optimization of Convective Heat Transfer from Two Heating Generators into Horizontal Enclosure Including A Discrete Obstacle: A Lattice Boltzmann Comprehensive Investigation

T. Naffouti<sup>1,2,3,†</sup>, L. Thamri<sup>1,4</sup>, A. Naffouti<sup>1,4</sup> and J. Zinoubi<sup>1,2,3</sup>

<sup>1</sup> *University of Tunis El-Manar, Faculty of Sciences of Tunis, Department of Physics, Tunisia*

<sup>2</sup> *Laboratory of Energizing and Thermal and Mass Transfers, El Manar 2092, Tunis, Tunisia*

<sup>3</sup> *Preparatory Institute of the Engineers Studies of El-Manar, El-Manar 2092, Tunis, Tunisia.*

<sup>4</sup> *Laboratory of fluid mechanics and Thermal Transfers, El Manar 2092, Tunis, Tunisia*

†Corresponding Author Email: [taoufiknaffouti@gmail.com](mailto:taoufiknaffouti@gmail.com)

(Received November 25, 2017; accepted April 6, 2018)

## ABSTRACT

This paper is intended to address the effect of a discrete obstacle on the behavior of flow and heat transfer of laminar natural convection in horizontal enclosure heated from below and symmetrical cooled from sides. Horizontal walls of the enclosure are considered adiabatic except the obstacle. Heating generators of a rectangular form and localized symmetrically are heated at a same uniform temperature. The cold obstacle is placed between active generators that create two thermal plumes. The double population lattice Boltzmann with standard models D2Q9 and D2Q4 for flow and temperature is used to simulate the problem. Prandtl number (Pr), Grashoff number (Gr) and aspect ratio of the enclosure (A) are fixed to 0.71,  $10^5$  and 2, respectively. Computational results are performed for pertinent geometric parameters of the obstacle in the following ranges: height  $0 \leq H_o \leq 0.75$ , position  $0 \leq X_{co} \leq 0.5$  and length  $0.1 \leq L_o \leq 0.6$ . It is found that predicted results with LBM are in line with previous investigations. Simulations show that adding the obstacle inside an enclosure conduct to change considerably the thermo-fluid characteristics. Hence, increasing the obstacle height causes a destruction of the interference between thermal plumes. On the other hand, optimum of heat transfer is discovered for a centred obstacle ( $X_{co} = 0$ ) and for smaller length and greatest height of this one.

**Keywords:** Lattice Boltzmann method; Convective heat transfer; Horizontal enclosure; Discrete obstacle; Optimization of heat transfer.

## NOMENCLATURE

A	aspect ratio of the enclosure	Nu*(H1)	Nusselt number ratio along horizontal hot upper wall of generator S <sub>1</sub>
c <sub>s</sub>	lattice sound speed	Nu*(H2)	Nusselt number ratio along horizontal hot upper wall generator S <sub>2</sub>
c <sub>i</sub>	discrete lattice velocity	Nu*(VL1)	Nusselt number ratio along vertical left hot wall of generator S <sub>1</sub>
f <sub>i</sub>	discrete distribution function for the density	Nu*(VR1)	Nusselt number ratio along vertical right hot wall of generator S <sub>1</sub>
g <sub>i</sub>	discrete distribution function for the temperature	Nu*(VL2)	Nusselt number ratio along vertical left hot wall of generator S <sub>2</sub>
g	gravity field	Nu*(VR2)	Nusselt number ratio along vertical right hot wall of generator S <sub>2</sub>
H <sub>o</sub>	dimensionless height of the obstacle	$\beta$	thermal expansion coefficient
H <sub>e</sub>	dimensionless height of the enclosure	$\theta$	dimensionless temperature field
L <sub>e</sub>	dimensionless length of the enclosure	w <sub>i</sub>	weighting factors for f <sub>i</sub>
L <sub>o</sub>	dimensionless length of the obstacle	w <sub>i</sub>	weighting factors for g <sub>i</sub>
$\Delta T$	temperature gradient		
$\Delta t$	time step		
T <sub>h</sub>	temperature of hot source		
T <sub>c</sub>	temperature of cold vertical wall		
$\Delta x$	lattice spacing units (=Δy)		
Gr	Grashoff number		
u	velocity vector (u <sub>x</sub> ,v <sub>y</sub> )		

X<sub>co</sub> dimensionless position of the obstacle  
 X lattice node in (x,y) coordinates  
 Eq equilibrium part  
 H hot  
 abs absence  
 prs presence

$\tau_f$  relaxation times for f  
 $\tau_g$  relaxation times for g;  
 $\rho$  fluid density  
 $\nu$  kinetic viscosity  
 $\chi$  thermal diffusivity

## 1. INTRODUCTION

Natural convection heat transfer in confined medium is relevant in many thermal engineering applications in both nature and industry. Some examples include the thermal design of building, cooling devices in electronic equipment (Kim *et al.* (1996)), and heat exchanger apparatus, among others (Bose *et al.* (2013), Bao *et al.* (2015), Sankar *et al.* (2016), Saglam *et al.* (2018)). Natural convection cooling is widely used due to its simplicity, high reliability, absence of noise and low maintenance cost (Peterson *et al.* (1990), Aydin *et al.* (2000)). The literature show that several experiments and numerical approaches are presented to describe the phenomenon of natural convection in enclosures heated from below. Mantle J. *et al.* (1994) performed an experimental investigation on effect of wall temperature modulation in a horizontal fluid layer heated from below. After that, Papanicolaou E. and Gopalakrishna S. (1995) carried out a numerical study of natural convection created in a horizontal, enclosed air heated from below by a discrete heater at a uniform heat flux. The flow is very affected by aspect ratio and source size. Then, Ortega A. and B. S. Lall (1996) performed experiments to measure the heat transfer coefficient on the surface of a square flush-mounted heat source at the center of a plate in a small horizontal enclosure. Soong C. Y. *et al.* (2001) are focused their attention on thermal-fluid behaviors in a rectangular enclosure heated from below with wall-temperature varied sinusoidally. By studying the interaction between discrete heat sources in horizontal natural convection enclosures with a finite volume method, Qi-Hong D. *et al.* (2002) concluded that characteristics of the fluid flow and heat transfer are much related to the separation distance between heaters. Natural convection from narrow horizontal plates versus moderate Rayleigh numbers experimentally is investigated by Martorell I. *et al.* (2003). They proved that the Nusselt number does not significantly depend with the aspect ratio of a horizontal plate cooled from above. Tso C. P. *et al.* (2004) carried out experimental and numerical investigations of laminar natural-convection cooling of water in a rectangular enclosure of nine heaters with different inclinations. It is found that the heat transfer is significant for the case of horizontal cavity heated from below. Bazylak A. *et al.* (2006) studied natural convection in an enclosure with distributed heat sources using code fluent. They showed that heat transfer rates increase as the spacing length between sources increase. Naffouti T. and R.

Djebali (2012) performed a computational investigation on natural convection flow and heat transfer in square enclosure asymmetrically heated from below with LBM. They concluded that increasing the hot source length affects greatly thermal and dynamic fields as well as the heat transfer rate. Using code fluent, Kusammanavar B. *et al.* (2012) simulated the effect of heat source location on natural convection in a square cavity. For various Rayleigh numbers, they demonstrated that heat transfer is considerable where hot sources are located at different positions. After that, Naffouti T. *et al.* (2013) applied lattice Boltzmann method to simulate 2-D natural convection heat transfer in a square enclosure symmetrical cooled from the sides and including a rectangular heat block located on the bottom wall. Graphical results in term of streamlines and isotherms are strongly affected by Rayleigh number, position, length and height of the active block.

From the available literature, a few research papers are published on the enhancement of heat transfer of natural convection in confined medium. For example, Cho C.C *et al.* (2012) simulated the enhancement of convective heat transfer in enclosure containing a nanofluid of Al<sub>2</sub>O<sub>3</sub>-water with finite-volume method. It is proved that heat transport increases with the volume fraction of nanoparticles. Moradi H. *et al.* (2015) carried out an experimental study on characterization and optimization of natural convection heat transfer of two Newtonian Al<sub>2</sub>O<sub>3</sub>/water and TiO<sub>2</sub>/water nano-fluids in a cylindrical enclosure. They showed that adding nano-particles to water conduct to a slight increase of convective heat transfer. In the same period, Bao Y *et al.* (2015) performed an experimental and numerical study on the enhancement of convective heat transfer in partitioned cavity. They found that the presence of partition walls conduct to enhance the heat transport than that of un-finned cavity. Using LBM, Naffouti T. *et al.* (2016) performed a numerical study on the optimization of convective heat transfer inside an enclosure heated by the bottom with two active blocks. Computations results show that the maximum of heat transfer rate is obtained for the case of square enclosure and for heaters localized in the vicinity of vertical cold walls. Elsayed R. F. *et al.* (2016) are interested to optimization of natural convection heat transfer from a horizontal finned tube. Experimental results show that the convection heat transfer rate increases with increasing fin diameter.

The enhancement of heat transfer by natural

convection is an interesting topic for different kinds of industrial and engineering applications. Hence, LBM is applied to evaluate flow characteristics and heat transfer of natural convection in a rectangular enclosure heated from below while adding a discrete obstacle localized between two heating generators. For a fixed Grashoff number at  $10^5$ , effects of height, position and length of the obstacle on the flow and heat transfer systematically are examined.

## 2. MATHEMATICAL FORMULATION

### 2.1 Physical Configuration

The configuration, coordinate system and boundary conditions of the 2-D problem under consideration are illustrated schematically in Fig. 1. It concerns a natural convection of air in a rectangular enclosure ( $A = L_e/H_e$ ) of height  $H_e$  and length  $L_e = 2 H_e$  heated from below with two identical heating generators and symmetrically cooled from sides at a constant low temperature  $T_c$ . Centers positions of fixed hot sources  $S_1$  and  $S_2$  are located at  $X_{CS1} = 0.15$  and  $X_{CS2} = 0.85$ , respectively. Length and height of each active source are 0.1 and 0.05. The confined fluid is assumed incompressible, Newtonian and the flow is considered laminar. Between hot generators maintained at a uniform hot temperature  $T_h$  is localized a rectangular obstacle of length  $L_o$  and height  $H_o$ . All obstacle walls are isothermally cooled at a constant temperature  $T_c$  and horizontal walls of the enclosure are insulated except the obstacle and heaters. To exam the effect of a discrete obstacle on convective heat transfer in the enclosure, computations with LBM are performed through the variation of geometrical parameters of the obstacle; height  $H_o$  from 0 to 0.75, length  $L_o$  from 0.1 to 0.6 and position  $X_{CO}$  from 0 to 0.5.

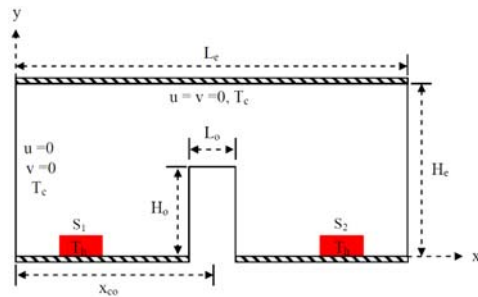


Fig. 1. Schematic diagram of the physical problem

### 2.2 Numerical method of Lattice Boltzmann

To simulate the incompressible thermal problem, LBM is used in this work with standard two dimensional, nine velocities D2Q9 for flow and four velocities D2Q4 for temperature (Naffouti T. *et al.* (2013), Naffouti T. *et al.* (2016)). Therefore, only brief discussion will be given in the following paragraphs, for completeness. In this model, double distribution function thermal

lattice Boltzmann introduced by He X. (1997) with single relaxation time (SRT) resulting from the Bhatnagar-Gross-Krook (BGK) approach for the collision operator.

For the flow field, distribution function in lattice Boltzmann SRT model is written as:

$$f_i(x + c_i \Delta t, t + \Delta t) - f_i(x, t) = \frac{1}{\tau_f} [f_i(x, t) - f_i^{eq}(x, t)] + \Delta t F_i \quad (1)$$

where  $f_i$  is the particle distribution introduced for the finite set of the discrete particle velocity vectors  $c_i$ . The  $\tau_f$  and  $f_k^{eq}$  noted the relaxation time of the BGK approximation and the equilibrium distribution function, are respectively given as:

$$\tau_f = 3\nu + 0.5 \quad (2)$$

where  $\nu$  is the kinematic viscosity of the flow.

$$f_i^{eq} = w_i \rho \left[ 1 + \frac{c_i u}{c_s^2} + \frac{1}{2} \frac{(c_i u)^2}{c_s^4} - \frac{1}{2} \frac{u^2}{c_s^2} \right] \quad (3)$$

$c_s = \frac{c}{\sqrt{3}}$  is the speed of sound,  $c = \frac{\Delta x}{\Delta t}$  is the lattice streaming speed.  $\Delta x$  and  $\Delta t$  are the lattice space and the lattice time step size, respectively, which are set to unity.

Weighting  $w_i$  for D2Q9 model are given as

$$w_0 = \frac{4}{9}, w_{1-4} = \frac{1}{9}, w_{5-8} = \frac{1}{36}$$

Discrete velocities  $c_i$  are defined as:  $c_0 = (0, 0)$ ,  $c_{1-4} = (\pm c, 0)$  and  $c_{5-8} = (\pm c, \pm c)$ .

For D2Q9 model,  $u$  and  $\rho$  are the macroscopic velocity vector and density, respectively.

In the present investigation, the Boussinesq approximation is applied in order to model buoyancy force in the flow field. Hence, the external force term in each direction can be defined as:

$$F_i = 3w_i g \beta \Delta T \quad (4)$$

Where  $\Delta T$ ,  $g$  and  $\beta$  are temperature difference, gravitational acceleration and thermal expansion coefficient, respectively.

Hydrodynamic variables  $u$  and  $\rho$  are obtained through moment summations in the velocity space:

$$[\rho, \rho u] = \sum_{i=0}^8 [f_i, c_i f_i] \quad (5)$$

For the temperature field, another distribution function in lattice Boltzmann SRT model ( $g_i$ ) is defined as:

$$g_i(x + c_i \Delta t, t + \Delta t) - g_i(x, t) = -\frac{1}{\tau_g} [g_i(x, t) - g_i^{eq}(x, t)] \quad (6)$$

For scalar function related to temperature, the single relaxation time  $\tau_g$  and the equilibrium distribution function  $g_i^{eq}$  can be expressed as:

$$\tau_g = 2\chi + 0.5 \quad (7)$$

where  $\chi$  is the thermal diffusivity of the flow.

$$g_i^{eq} = w_i' \theta \left[ 1 + \frac{c_i \cdot u}{c_s^2} \right] \quad (8)$$

$w_k' = 0.25$  is the temperature weighting factor for each direction of D2Q4 model.

The dimensionless temperature  $\theta$  is calculated by summing the distribution functions over the four-velocity directions, as:

$$[\theta] = \sum_{i=1}^4 [g_i] \quad (9)$$

Using the incompressible flow,  $Ma = |u|/c_s \ll 1$  and the Chapman-Enskog expansion (He X. and Luo L.S (1997)), governing equations of continuity, momentum and energy can be derived from discrete lattice Boltzmann equations.

### 2.3 Boundary Conditions in LBM

To carried out a numerically study on natural convection problems with LBM, the implementation of boundary conditions is a necessary step. Distribution functions out of the computation domain are known with the streaming process. Unknown distribution functions are those toward the domain (Fig. 2).

For the flow with D2Q9 model, a conventional bounce-back boundary conditions is applied on the solid boundaries (Naffouti T. *et al.* (2012), Mohamad A. A. *et al.* (2009)) which means that incoming boundary populations equal to out-going populations after collision. In the present investigation, following conditions are applied in the south and east walls, respectively:

$$f_{2,0} = f_{4,0}, f_{5,0} = f_{7,0}, f_{6,0} = f_{8,0} \quad (10)$$

$$f_{3,n} = f_{1,n}, f_{6,n} = f_{8,n}, f_{7,n} = f_{5,n} \quad (11)$$

where n is the lattice on the boundary.

For the temperature with D2Q4 model, adiabatic

boundary condition is applied on north and south boundary except the obstacle and two hot generators. The adiabatic boundary condition is transferred to Dirichlet-type condition using the conventional second-order finite difference approximation as:

$$g_{wall} = (4g_1 - g_2)/3 \quad (12)$$

The temperature at the west/east walls of the enclosure and all walls of the obstacle is clear, therefore  $\theta = 0$ . So, the distribution function  $g_1$ , for the west wall of the enclosure is given as:

$$g_{1,0} = -g_{3,0} \quad (13)$$

For all walls of each hot generator, the temperature is considered constant  $\theta = 1$ . For example, the boundary condition applied on horizontal hot wall is:

$$g_2 = 0.5 - g_4 \quad (14)$$

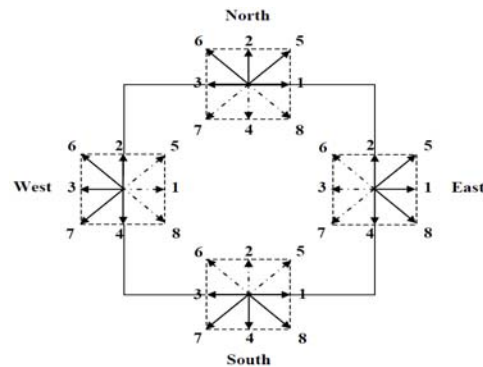


Fig. 2. Unknown and known distribution functions at the domain boundaries

### 2.4 Dimensionless Parameters

In order to study the incompressible thermal problem with the LBM, it is necessary to use a characteristic velocity  $U = \sqrt{g\beta\Delta TH_e}$  and then to calculate the corresponding kinetic viscosity ( $\nu$ ) and thermal diffusivity ( $\chi$ ) with the following equations related to Grashoff number (Gr) and Prandtl number (Pr), respectively:

$$\nu = \sqrt{\frac{U^2 H_e^2}{Gr}} \quad (15)$$

$$\chi = \frac{\nu}{Pr} \quad (16)$$

Grashoff number is defined as:

$$Gr = \frac{g\beta\Delta TH_e}{\nu^2} \quad (17)$$

To quantify the convective heat transfer inside the enclosure, it is crucial to calculate the Nusselt number along each hot wall of two heaters. Using a second order finite difference

scheme, average Nusselt number  $Nu_{hl}$  along horizontal hot upper wall of heater  $S_1$  is determinate by the following relation:

$$Nu_{hl} = \frac{1}{\mathcal{E}} \sum \frac{3\theta_0 - 4\theta_1 + \theta_2}{2} \quad (18)$$

where  $\mathcal{E}$  is the dimensionless length of hot wall.

The Nusselt number ratio along each hot wall is given by:

$$Nu^* = \frac{Nu(prsobstacle)}{Nu(absobstacle)} \quad (19)$$

The following convergence criterion was adopted for all dependent variables at each point in the computation domain:

$$\left| \frac{\Phi(t+\Delta t) - \Phi(t)}{\Phi(t)} \right| \leq 10^{-4} \quad (20)$$

where  $\Phi$  stands for a dependent variables  $\theta$ ,  $u_x$  and  $v_y$ .

### 3. RESULTS AND DISCUSSION

In the present study, the air was considered as a working fluid and the Prandtl number was taken  $Pr = 0.71$ . Thermal fields, dynamic fields and heat transfer rates along each hot wall inside the enclosure will be analyzed in the following sections for various geometrical parameters of the obstacle: height ( $0 \leq H_o \leq 0.75$ ), length ( $0.1 \leq L_o \leq 0.6$ ) and position ( $0 \leq X_{co} \leq 0.5$ ). For all results obtained with LBM, aspect ratio of the enclosure and Grashoff number are fixed at  $A = 2$  and  $Gr = 10^5$ , respectively.

#### 3.1 Validation of the Present Code and Grid Independence

In order to check on the accuracy of LB code employed for the solution of the considered problem, the present numerical code is validated against (view Naffouti T. *et al.*(2016)) with the published investigation of Raji A. *et al.* (1997) on the natural convection in interacting cavities heated from below. This study is carried out for aspect ratio  $A = 1.5$ , inclination angle  $\Phi = 0^\circ$  and the Prandtl number is fixed at 0.72. Figures 3 and 4 illustrate isotherms and streamlines of the flow predicted by our LB code and compared with predictions of finite difference method (DF) for various Rayleigh number (Ra) and obstacle height (B). It is found that thermal and dynamic fields of the flow for both methods gave same results. Hence, it is concluded that LBM with the suggested boundary conditions can produce reliable results. For all numerical computations with LBM, a uniform grid size of lattices number is used; 150 lattices number for the y-direction, and for the x-direction, the number of lattices is equal to 225.

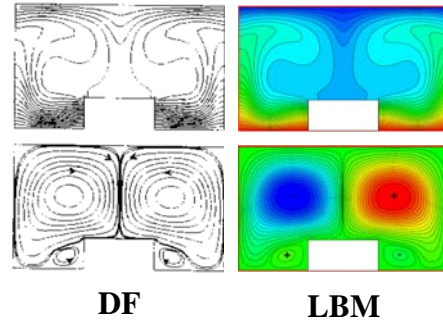


Fig. 3. Comparison of the present investigation (LBM) with that of Raji A. *et al.* (1997) (DF) for  $Ra = 10^5$  and  $B = 0.25$ : isotherms (top) and streamlines (bottom)

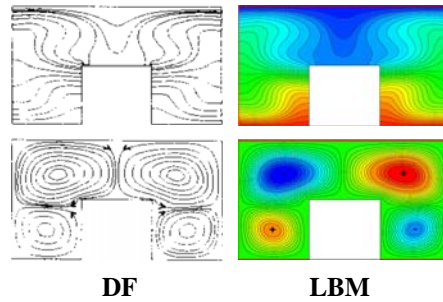


Fig. 4. Comparison of the present investigation (LBM) with that of Raji A. *et al.* (1997) (DF) for  $Ra = 6 \cdot 10^4$  and  $B = 0.5$ : isotherms (top) and streamlines (bottom)

In order to ensure the accuracy and reliability of results with LB code, tests are performed to determine the grid dependence of the flow and heat transfer characteristics. Numerical results with the present code are essentially dependent upon a judicious choice of grid size of the computational domain, i.e., rectangular. Figure 5 illustrate the grid size effect on the Nusselt number ratio ( $Nu^*$ ) predicted along each hot wall for both heating generators at fixed values of the aspect ratio ( $A = 2$ ), height obstacle ( $H_o = 0.6$ ), length obstacle ( $L_o = 0.1$ ), Grashoff number ( $Gr = 10^5$ ) and Prandtl number ( $Pr = 0.71$ ). The grid independence investigation is carried out for five uniform grid lattice sizes ranging from 15000 to 125000 lattices number. It can be seen that the grid size beyond 70000 elements is believed to be sufficiently refined enough to simulate correctly the problem. Therefore, numerical results by our LB code are carried out with grid size of 80000 elements.

#### 3.2 Detailed Convection Characteristics

##### 3.2.1 Effect of the Obstacle Height

Temperature and buoyant convection flow fields inside the enclosure with variation of the height ( $H_o$ ) of a centered obstacle are shown in terms of contour maps of isotherms and streamlines, respectively, as exemplified in Fig. 6. To consider only the effect of  $H_o$ , other parameters

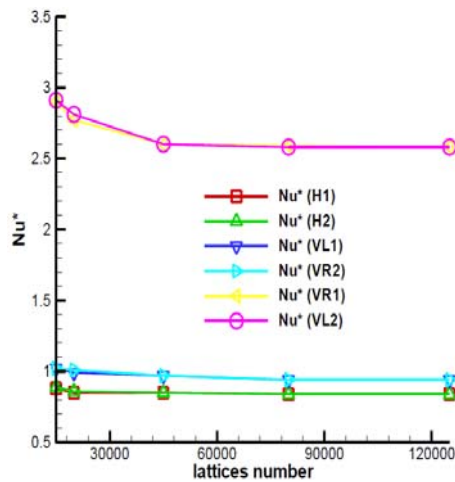


**Fig. 5. Influence of the lattices number on Nusselt number ratio for  $A = 2$ ,  $Gr = 10^5$ ,  $H_0 = 0.6$  and  $L_0 = 0.1$**

are kept constant as  $A = 2$ ,  $Gr = 10^5$  and  $L_0 = 0.1$ . As it can be seen from the figure, thermal and dynamic structures of the flow are symmetrical about the mid-length of the enclosure by the reason of symmetrical boundary conditions. In the absence of the obstacle related to  $H_0 = 0$ , the flow pattern is described by two counter-rotating cells in the left and right halves of the enclosure. Owing to buoyancy forces, the resulting flow of two thermal plumes generate by hot sources rises vertically toward adiabatic top wall, and then its moves symmetrically to cold walls. Due to effect of cooling, the flow descends along the corresponding cold wall in order to supply against heating generators by the bottom. Finally, a pair counter-rotating cells is generated with strong recirculation of the flow inside the enclosure owing to the dominance of convection heat transfer. From the figure, isotherms ( $H_0 = 0$ ) reveal higher values of the temperature in the central region between heaters under effect of a strong interaction of two thermal plumes. This physical phenomenon is indicated by available literature related to the interaction of thermal plume with surrounding environment (Bazylak A. *et al.* (2006), Naffouti T. *et al.* (2012), Kusammanavar B. *et al.* (2012)). More stratification of isotherms is observed in the vicinity of each cold wall. Also, it is found that a distortion of isotherms from cold walls of the enclosure toward central region due to the strong entrainment phenomenon of fresh air on exterior sides of active sources. A same conclusion is mentioned by many studies (Brahimi M. *et al.* (1989), Ichimiya K. *et al.* (2005), Mahmoud A. O. M. *et al.* (2007, 2008)). Therefore, results corresponding to the case of absence of the obstacle can demonstrate that the structure of resulting flow is nearly similar to that of thermal plume created by one heater localized in a confined space. In the presence of the obstacle related to  $H_0 = 0.25$ ,  $0.5$  and  $0.75$ , it may be noticed that the formation of two symmetrical secondary cells which develop at obstacle sides.

With increasing of the obstacle height, the recirculation of main cells becomes more weak and a move of their cores toward both top corners of the enclosure is detected. On the contrary, an acceleration of secondary cells is identified as the obstacle height increases. It implies an intensification of the entrainment of fresh air by the low in each region between the obstacle and hot source. However, the figure shows that thermal field is strongly affected by the variation of the obstacle height. Hence, the increase of the obstacle height causes an attenuation of the temperature of the flow in the region between heating generators owing to thermal boundary conditions of the obstacle. Consequently, a weakening of the interaction between two thermal plumes is concluded with increasing of  $H_0$ . For the higher obstacle height corresponding to  $H_0 = 0.75$ , it can be seen that the flow domain is equivalent of two identical enclosures separately by an obstacle where the communication of thermal plumes is negligible.

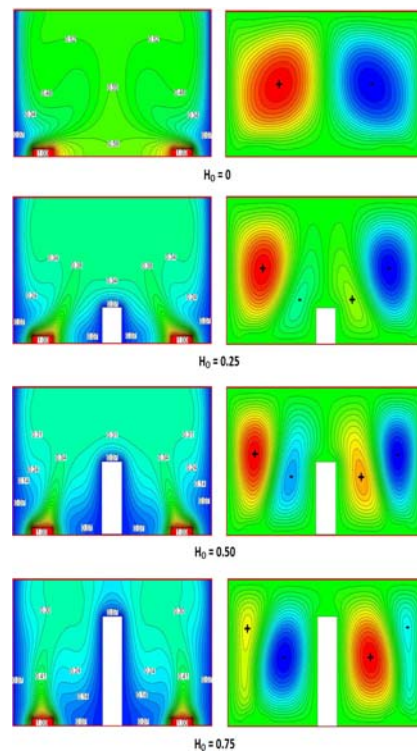


**Fig. 6. Behaviour of isotherms (left) and streamlines (right) vs. height of a centred obstacle  $H_0$  for  $L_0 = 0.1$**

### 3.2.2 Effect of the Obstacle Position

As mentioned before, characteristics of the flow are symmetrical in the presence of a centered obstacle corresponding to position  $X_{Co} = 0.5$ . For this configuration with  $H_0 = 0.75$  and  $L_0 = 0.1$ , flow pattern consists four cells and isotherms demonstrate that the interaction between thermal plumes is negligible. The present investigation shows that the obstacle position has a great effect on flow behavior into enclosure. On the Fig. 7 is presented the

influence of the obstacle position ( $X_{CO}$ ) upon isotherms and streamlines of the flow for  $H_O = 0.75$  and  $L_O = 0.1$ . Visual examination of this pertinent parameter ranging from  $X_{CO} = 0.45$  to  $0.3$  reveal a considerable variations among diverse configurations. From the figure, it is found that the flow and temperatures fields are described by an asymmetrical behavior for various positions  $X_{CO}$ . Seen from streamlines, a destruction of the dynamic field is detected with a deformation of different cells. As moving the obstacle to the left vertical wall of the enclosure, two secondary cells are formed close to other sides of this one. Hence, the flow pattern is characterized by five cells with different sizes at  $X_{CO} = 0.3$ . In addition, it is noticed an increases of the recirculation and the size of the cell near to the right vertical wall of the obstacle with the displacement of this one to the position  $X_{CO} = 0.3$ . On the contrary, the intensity of the recirculation and the size of two cells, in the region between the obstacle and the left cold wall of the enclosure, decreases with moving the obstacle toward  $X_{CO} = 0.3$ . These results prove an intensification of the entrainment of fresh air by the right heating generator. On the other hand, the figure shows that the thermal field of the flow is strongly affected by different positions of the obstacle. However, it is clear a significant deviation of the right thermal plume to the obstacle as moving this one to the left vertical wall of the enclosure. It is related to an intensification of the entrainment phenomenon indicated previously by the exam of streamlines. Furthermore, an attenuation of the temperature of the flow is showed by isotherms in the region between the left vertical wall of the enclosure and the obstacle with the displacement of this one to  $X_{CO} = 0.3$ . This finding demonstrates that the communication of thermals plumes become so weak particularly when the obstacle is localized close to the left vertical wall of the enclosure. Thus, the total enclosure with a discrete obstacle can be assimilated to an association of two small confined mediums which communicate only by the top.

### 3.2.3 Effect of the Obstacle Length

In order to better understanding the effect of the discrete obstacle on the behavior of the flow inside the enclosure, next attention is concentrated on the evolution of isotherms and streamlines versus obstacle length. Figure 8 depicts the effect of this parameter ranging from  $L_O = 0.1$  to  $0.4$  on thermal and dynamic fields of the flow for a centered obstacle with fixed height at  $H_O = 0.75$ . For different configurations, results show symmetrical repartitions of temperature and velocity about the mid-length of the enclosure. It is related to symmetrical boundary condition applied in this study. Also, the dynamic structure of the flow is described usually by four cells of various sizes. In addition, the increase of the obstacle length conducts to decrease the recirculation and the

size of two cells at sides of obstacle while an intensification of the rotation of cells closer to vertical walls of the enclosure is detected. Consequently, the entrainment of fresh air, by two heating sources, decreases near the obstacle with the increase of the length of this one. From isotherms, it is observed a strong deviation of both thermal plumes to cold walls of the enclosure thus indicating a phenomenon of a destructive interference between these latter as increasing the obstacle length. For higher length of the obstacle corresponding to  $L_O = 0.4$ , isotherms and streamlines show a weaker interaction between thermals plumes separated by the obstacle. For this configuration ( $L_O = 0.4$ ), it can be concluded that the behavior of the flow in each region between the obstacle and the cold wall of the enclosure is comparable to that of natural convection in a rectangular confined medium heated from below and symmetrically cooled from sides (Roychowdhury D. G. *et al.* (2002), Goutam S. *et al.* (2007), Paroncini M. *et al.* (2009), Khozaymehnezhad H. *et al.* (2012)).

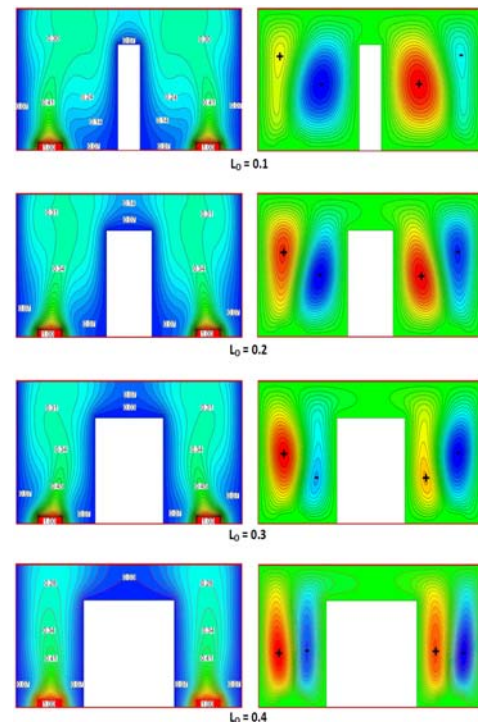


**Fig. 7. Behaviour of isotherms (left) and streamlines (right) vs. obstacle position  $X_{CO}$  for  $H_O = 0.75$  and  $L_O = 0.1$**

### 3.3 Optimization of Convective Heat Transfer

Next, consideration concerns the optimization of heat transfer of the flow in the presence of the discrete obstacle. This investigation can help to protect thermals systems and to control natural convection flow which propagates in confined medium. Generally, the Nusselt number is considered one of the most important engineering parameter to quantify heat transfer rates. For this reason, various evolution of the

Nusselt number ratio ( $Nu^*$ ) of the flow along each hot wall over the ranges of pertinent parameters of the obstacle; height ( $0 \leq H_o \leq 0.75$ ), position ( $0 \leq X_{co} \leq 0.5$ ) and length ( $0.1 \leq L_o \leq 0.4$ ) are presented and examined in the following sections.

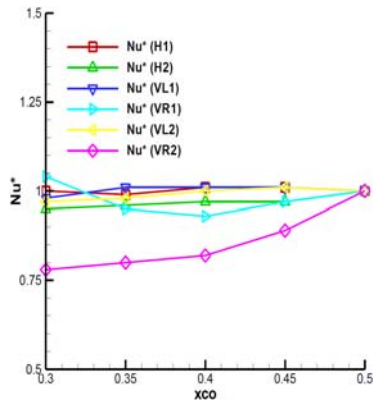


**Fig. 8. Behaviour of isotherms (left) and streamlines (right) vs. length of a centred obstacle  $L_o$  for  $H_o = 0.75$**

Figure 9 depicts the effect of the obstacle height  $H_o$  on the  $Nu^*$  for fixed position  $X_{co}$  and length of the obstacle at  $X_{co} = 0$  and  $L_o = 0.1$ , respectively. It can be seen from plots that heat transfer present the same evolution on each both symmetrical hot walls of heaters such as the variation of the Nusselt number ratio on horizontal hot walls noticed  $Nu^*(H1)$  and  $Nu^*(H2)$ . It is related to symmetrical boundary conditions applied in the present study. On the other hand, it is found that the increase of the height obstacle conduct to increase the  $Nu^*$  only along the vertical right hot wall of the heater  $S_1$  and the left hot wall of heater  $S_2$  noted  $Nu^*(VR1)$  and  $Nu^*(VL2)$ , respectively. Thus, it can be concluded that adding of a centered discrete obstacle with length of  $L_o = 0.1$  can improve the heat transfer of the flow inside horizontal enclosure with higher height at  $H_o = 0.75$ .

Plots of Nusselt number ratio on each hot wall with various obstacle positions ( $X_{co}$ ) are illustrated on the Fig. 10 with  $H_o = 0.75$  and  $L_o = 0.1$ . It can be observed that the heat transfer along vertical right hot wall of the active source  $S_2$ , noted  $Nu^*(VR2)$ , is strongly affected by the obstacle localization. Hence, the displacement of the obstacle to the left cold wall of the enclosure leads to decrease the  $Nu^*(VR2)$  thus indicating that the heat transfer is more significant for a centered obstacle corresponding to  $X_{co} = 0.5$ . On the other hand, the figure shows that the values of heat transfer rates are comparable and remain practically constant along other hot walls. On the Fig. 11 is presented the evolution of the Nusselt number ratio on each hot wall versus the length obstacle ( $L_o$ ) for fixed height and position of the obstacle at  $H_o = 0.75$  and  $X_{co} = 0.5$ . A fast growth of heat transfer rates related to  $Nu^*(VR1)$  and  $Nu^*(VL2)$  with the length of the obstacle is demonstrate from  $L_o = 0$  to 0.1, and then, it decreases slightly with the length to  $L_o = 0.4$ . Along other hot wall, it is found that values

of  $Nu^*$  are very weak and considered comparable. Consequently, it can be concluded that the heat transfer is enhanced for a length of obstacle equal to  $L_o = 0.1$ .

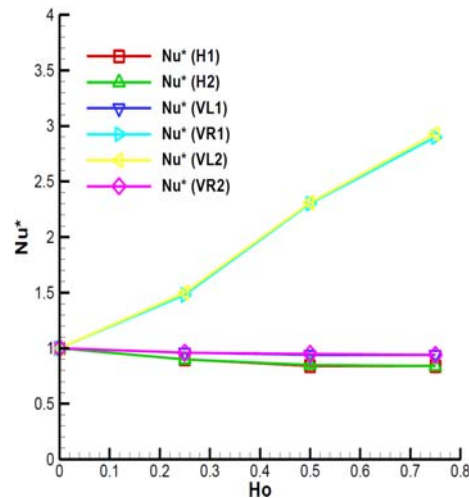


**Fig. 9. Dependence of the Nusselt number ratio along each hot wall of both heating generators on the height of a centered obstacle with  $L_o = 0.1$**

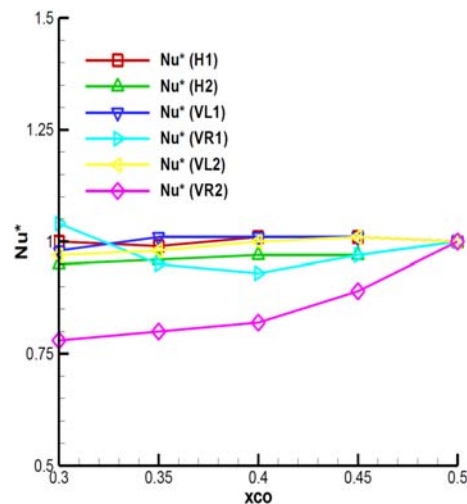


**Fig. 10. Dependence of the Nusselt number ratio along each hot wall of both heating generators on the obstacle position for  $H_o = 0.75$  and  $L_o = 0.1$**

### 5. CONCLUSION

The present investigation via LBM has been carried out to unveil the influence of a discrete obstacle on the natural convection flow into a horizontal enclosure cooled by sides and heated from below with two heating generators. Hence, the main focus of the problem is to find the adequate geometrical parameters of the obstacle in order to optimize the convective heat transfer inside the enclosure. For this reason, effects of parameters of the obstacle; height, position and length are assessed.

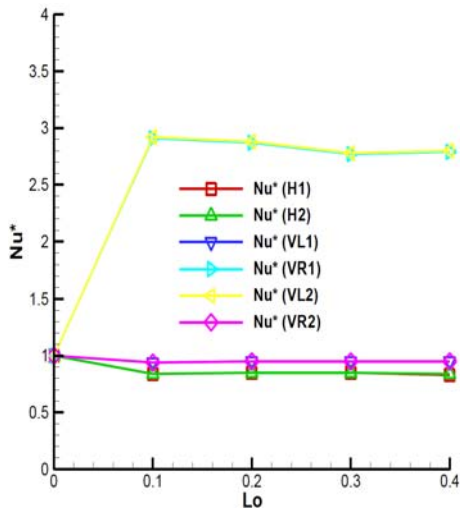


**Fig. 11. Dependence of the Nusselt number ratio along each hot wall of both heating generators on the length of a centered obstacle for  $H_o = 0.75$**

Essential findings obtained with LBM may be recap as follows:

- Results of LBM were validated with the DF, and a good agreement is concluded. So, it can be proved that the LBM is a powerful and suitable numerical method to solve many natural convection problems and heat transport phenomena.
- For the configuration corresponding to the absence of an obstacle ( $H_o = 0$ ), streamlines show that the flow pattern is described by two counter-rotating cells. Isotherms show a considerable interaction between thermal plumes. Thus, the resulting flow is nearly similar to that of thermal plume generated by one hot source positioned from below of rectangular enclosure.
- The addition of a discrete obstacle is advantageous for the flow and heat transfer into the enclosure, and its behaviors are complicated. Hence, thermal and dynamic fields are strongly influenced by the change of the height, position and length of the obstacle.
- The increase of height  $H_o$  and length  $L_o$  of the obstacle conduct to destroy the dynamic field of the flow and four cells are formed with different sizes and intensity recirculation.
- The interaction between thermal plumes becomes weaker for  $H_o = 0.75$ ,  $L_o = 0.4$  and a centered obstacle. Thus the enclosure can be assimilated to an association of two small confined spaces which communicate by the top.
- It is found a considerable deviation of the right thermal plume to the obstacle as moving this one to the left cold wall of the enclosure and five cells with various sizes are formed particularly at  $X_{co} = 0.3$ .
- Heat transfer is enhanced with the growth of the height to  $H_o = 0.75$  and the length of the

obstacle to  $L_o = 0.1$ .

- As we move the obstacle to the left wall of the enclosure, the Nusselt number ratio decreases. Consequently the heat transfer is more important for a centered obstacle.
- For  $Gr = 10^5$  and  $A = 2$ , the optimization of convective heat transfer is obtained for a centered obstacle with higher height and smaller length at  $H_o = 0.75$  and  $L_o = 0.1$ , respectively.

## REFERENCES

- Aydin, O., J. Yang, (2000), Natural convection in enclosure with localized heating from below and symmetrically cooling from sides, *International Journal of Numerical Methods of Heat and Fluid Flow*. (10), 518-529.
- Bose, P. K., D. Sen, R. Panua and A. K. Das, (2013), Numerical Analysis of Laminar Natural Convection in a Quadrantal Cavity with a Solid Adiabatic Fin Attached to the Hot Vertical Wall, *Journal of Applied Fluid Mechanics*. (6), 501-510.
- Bao, Y., J. Chen, BF. Liu, Z.S. She, J. Zhang and Q. Zhou, (2015), Enhanced heat transport in partitioned thermal convection, *Journal of Fluid Mechanics*. (784), 1-11.
- Bazylak, A., N. Djilali, and D. Sinton, (2006), Natural convection in an enclosure with distributed heat sources, *Numerical Heat Transfer, Part A*. (49), 655-667.
- Brahimi, M., L. Dehmani and D. K. Son. (1989), Structure turbulente de l'écoulement d'interaction de deux panaches thermiques, *International Journal of Heat and Mass Transfer*. (32), 1551-1559.
- Cho, C.C., H.T. Yau and C.K. Chen, (2012), Enhancement of natural convection heat transfer in a u-shaped cavity filled with  $Al_2O_3$ -water nanofluid, *Thermal Science*. (16), 1317-1323.
- Elsayed, R. F., M. K. Elriedy, E. A. E lkady, Mustafa Ali, (2016), Natural Convection Heat Transfer Optimization From A Horizontal Finned Tube, *Journal of Multidisciplinary Engineering Science and Technology*. (3), 6141-6150.
- Goutam, S., S. Sumon, M. Quamrul Islam and M. A. Razzaq Akhanda, (2007), Natural convection in enclosure with discrete isothermal heating from below, *Journal of Naval architecture and marine engineering*. (4), 1-13.
- He, X. and L.S. Luo, (1997), Lattice Boltzmann Model for the incompressible Navier-Stokes equation, *Journal of statistical Physics*. (88), 927-944.
- Ichimiya, K., and H. Saiki, (2005), Behavior of thermal plumes from two-heat sources in an

- enclosure, *International Journal of Heat and Mass Transfer*. (48), 3461–3468.
- Khozayemnezhad, H., S. A. Mirbozorgi, (2012), Comparison of natural convection around a circular cylinder with a square cylinder inside a square enclosure, *Journal of Mechanical Engineering and Automation*. (2), 176-183.
- Kim, S.J. and S.W. Lee, (1996), Air cooling technology for electronic equipment, CRC Pres, Boca Raton, LA.
- Kusammanavar, B., K. S. Shashishekar and K. N. Seetharamu, (2012), Effects of heat source location on natural convection in a square cavity, *International Journal of Engineering Research & Technology*.(1), 1-8.
- Mahmoud, A. O. M., J. Bouslimi and R. Ben Maad, (2008), Experimental study of the effects of a thermal plume entrainment mode on the flow structure: Application to fire, *Fire Safety Journal*. (44), 475-486.
- Mahmoud, A. O. M., J. Zinoubi and R. Ben Maad, (2007), Study of hot air generator with quasi-uniform temperature using concentrated solar radiation: Influence of the shape parameters, *Renewable Energy*. (32), 351-364.
- Mantle, J., M. Kazmierczak, and B. Hiawy, (1994), The Effect of temperature modulation on natural convection in a horizontal layer heated from below: High Rayleigh number experiments, *Journal of Heat Transfer*. (116), 614–620.
- Martorell, I., J. Herrero, and F. X. Grau, (2003), Natural Convection from Narrow Horizontal Plates at Moderate Rayleigh Numbers, *International Journal of Heat and Mass Transfer*. (46), 2389-2402.
- Mohamad, A. A. , M. El-Ganaoui , R. Bennacer , (2009), Lattice Boltzmann simulation of natural convection in an open ended cavity, *International Journal of Thermal Sciences*. (48), 1870–1875.
- Moradi, H. , B. Bazooyar , A. Moheb, S. Gholamreza Etemad, (2015), Optimization of natural convection heat transfer of Newtonian nanofluids in a cylindrical enclosure, *Chinese Journal of Chemical Engineering*. (23), 1266–1274.
- Naffouti, T. and R. Djebali, (2012), Natural convection flow and heat transfer in square enclosure asymmetrically heated from below: A lattice Boltzmann comprehensive study, *Computer Modeling in Engineering and Sciences*. (88), 211-227.
- Naffouti, T., J. Zinoubi and R. Ben Maad, (2013), Lattice Boltzmann Analysis of 2-D Natural Convection Flow and Heat Transfer within Square Enclosure including an Isothermal Hot Block, *International Journal of Thermal Technologies*. (3), 146-154.
- Naffouti, T., J. Zinoubi, N. A. Che Sidik and R. B. Maad, (2016), Applied Thermal Lattice Boltzmann Model for Fluid Flow of Free Convection in 2-D Enclosure with Localized Two Active Blocks: Heat Transfer Optimization, *Journal of Applied Fluid Mechanics*. (9), 419-430.
- Ortega, A. and B. S. Lall, (1996), Natural convection air cooling of a discrete source on a conducting board in a shallow horizontal enclosure, *Twelfth IEEE SEMI-THERM Symp*, 201-213.
- Papanicolaou, E. and S. Gopalakrishna, (1995), Natural convection in shallow horizontal air layers encountered in electronic cooling, *Journal Electronic Packaging*. (117), 307–316.
- Paroncini, M., F. Corvaro, (2009), Natural convection in a square enclosure with a hot source, *International journal of thermal sciences*. (48), 1683-1695.
- Peterson, G.P. and A. Ortega, (1990), Thermal control of electronic equipment and devices, *Advances in Heat Transfer*. (20), 181-214.
- Qi-Hong, D. , T. Guang-Fa , L. Yuguo , H. Man Yeong , (2002) ,Interaction between discrete heat sources in horizontal natural convection enclosures, *International Journal of Heat and Mass Transfer*. (45), 5117-5132.
- Raji, A., M. Hasnaoui and Z. Zrikem, (1997), Natural convection in interacting cavities heated from below, *International journal of numerical methods for heat and fluid flow*. (7), 580-597.
- Roychowdhury, D. G., S. K. Das, T. S. Sundararajan, (2002), Numerical simulation of natural convective heat transfer and fluid flow around a heated cylinder inside an enclosure, *Heat and mass transfer*. (38), 565-576.
- Sankar, M., B. V. Pushpa, B. M. R. Prasanna and Y. Do, (2016), Influence of Size and Location of a Thin Baffle on Natural Convection in a Vertical Annular Enclosure, *Journal of Applied Fluid Mechanics*. (9), 2671-2684.
- Saglam, M., B. Sarper and O. Aydin, (2018), Natural Convection in an Enclosure with a Discretely Heated Sidewall: Heatlines and Flow Visualization, *Journal of Applied Fluid Mechanics*. (11), 271-284.
- Soong, C. Y., P. Y. Tzeng, and C. D. Hsieh, (2001), Numerical Study of Bottom-Wall Temperature Modulation Effects on Thermal Instability and Oscillatory Cellular Convection in a Rectangular Enclosure, *International Journal of Heat and Mass Transfer*. (44), 3855-3868.
- Tso, C. P., L. F. Jin, S. K. W. Tou, and X. F. Zhang, (2004), Flow pattern in natural convection cooling from an array of discrete heat sources in a rectangular cavity at various orientations, *International Journal of Heat and Mass Transfer*. (47), 4061-4073.